

## XPS STUDY OF EXPOSE TO AIR Cu-ISE SENSING MEMBRANE SURFACE

M. ESSI<sup>a,\*</sup>, B. KEDI<sup>b</sup>

<sup>a</sup>*Laboratoire de Chimie des Matériaux Inorganiques, Université Félix HOUPHOUET-BOIGNY de Cocody, UFR-SSMT, 22 BP 582 Abidjan 22, Côte d'Ivoire*

<sup>b</sup>*Laboratoire des Sciences et Technologies de l'Environnement, Université Jean Lorougnon GUEDE de Daloa, UFR Environnement, BP 150 Daloa, Côte d'Ivoire*

Cu [Ge<sub>28</sub>Sb<sub>12</sub>Se<sub>60</sub>]<sub>1-x</sub> thin films were prepared on Si substrates by using RF co-sputtering technique. The compositions were proved to be reproducible with no change in composition throughout the sample. The microstructure shows the presence of the columnar structure. SEM, EDS and SIMS indicated that the layers were homogeneous and were poorly contaminated. A XPS analysis of the surface was then undertaken in order to study the effects of the storage on sensor behavior. An oxidation caused by exposure to air of the thin films were studied by using X-ray photoelectron spectroscopy (XPS). Chemical composition analysis of XPS spectra revealed that oxygen detected on the film surfaces was increased with Sb<sub>2</sub>O<sub>5</sub> species formation.

(Received October 17, 2018; Accepted January 12, 2019)

**Keywords:** Chalcogenide glass, RF Sputtering, X-ray photoelectron spectroscopy (XPS), Copper-selective electrode (Cu-SE), Thin film

### 1. Introduction

Today the rapid detection of Pollutant has become important for environmental monitoring. This implies an increasing number of demands for more sensitive devices, capable of realtime species detection. Therefore integrated devices are increasingly being used for chemical sensing applications. Heavy metal ions are ones of the most toxic species of superficial and ground waters [1]. It is well established that ion-selective electrodes (ISEs) potentiometry can be used in the measurement of the activity of an individual ion. ISEs are sensors that undergo selective sensing at the surface due to chemisorption. Moreover, It has been established that ion-selective electrodes (ISEs) offer an alternative method for the electroanalysis of metal species in environmental samples [2–6]. Use of chalcogenide glasses as the membrane material for these chemical sensors makes them suitable for the detection of many chemical species in solution at concentrations lying in the ppm range [7-9]. Recently, considerable interest is attracted by the chemical microsensors which is closely connected with the trends of device miniaturization, ecology of the production and natural raw materials economy [10–13]. The thin films possess significantly lower potential compared to the corresponding bulk materials, which is required for glasses with low conductivity to be applied in the microsensors. This requirement is met by a wide range of chalcogenide glassy Alloys. In addition, their electrical properties can be adjusted by doping control. Chalcogenide and chalco-halide glass-forming systems have been investigated as membrane materials for chemical sensors, microsensors and multisensor systems. Most of the investigated Chalcogenide ISEs are characterized with linear electrode functions in a wide concentration range of the primary ion [14-17]. Most importantly, the chalcogenide glass was shown to be chemically more stable compared to its crystalline counterpart [18-21]. In the common case, such sensors are applicable at pH < 8 and also in strong redox electrolytes, but ion sensitive membranes are not stable and dissolve in alkaline media [22, 23]. Generally, Chalcogenide ISEs exhibit stable electrode function only after conditioning in the concentrated

---

\*Corresponding author: marc.essi@netcourrier.com

solutions of the potential-determining ion, which is probably connected with the formation of an active modified surface layer (MSL) [6, 7, 24]. The response time varies drastically with the membrane composition from few seconds to about a minute and it is determined by the diffusion coefficients of the potential-determining ions from the solution to the active centers in the MSL [7]. As a rule, Chalcogenide materials are reversible to the metal ions which are included in the composition of the glassy alloy [25, 26].

The wide-cross sensitivity combined with good chemical durability make Chalcogenide devices suitable components in multisensor systems, so called “electronic tongue”. A majority of previous work concerned the realisation of an ion-selective electrode for the detection of copper (II) in solutions. Since Jasinski et al. [26] other systems had been investigated [14-17, 27-34]. Other way with the deposition by RF sputtering experiment of a chalcogenide materials had been developed [19, 35-37]. Previous paper reports some investigation of the studied device lifetime tested in water site conditions for the copper detection [7]. XPS clearly shown that the chemical composition of the surface is modified as soon as the membrane is soaked in a copper (II) solution and its alteration corresponds to an oxidation of the membrane surface. In fact, more than one month is needed to see a quasitotal oxidation of the membrane and the end-of-life of the sensor. Subsequently, the present study of the  $\text{Cu}_x [\text{Ge}_{28}\text{Sb}_{12}\text{Se}_{60}]_{1-x}$  chalcogenide glass membrane was deemed appropriate in order to investigate the micro-sensor surface. More especially XPS investigation on air-exposed thin films was aimed to study influence of storage on ISE out-put signal and life-time.

## 2. Experimental

After a bibliographic and experimental study the composition  $\text{Cu}_x [\text{Ge}_{28}\text{Sb}_{12}\text{Se}_{60}]_{1-x}$  was selected [19, 27, 27]. Thin films of sensitive materials were prepared by RF co-sputtering of IG5 VITRON commercial target (i.e.  $\text{Ge}_{28}\text{Sb}_{12}\text{Se}_{60}$ ) and copper metal assembled as a composite target as shown in figure 1. An Alcatel Dion 300 device equipped with a PFG 300 RF Huttinger, 13.56 MHz, 300 W generator was used. Before the deposition, the chamber was evacuated down to approximately  $10^{-6}$  Pa to avoid ambient contamination. Nano films were elaborated under Argon plasma. Argon pressure was fixed to  $10^{-2}$  mbar. A low power of 25 W was fixed because of the dielectric character of the chalcogenide matrix. The sensing film was deposited over a microscope slide substrate covered with a chromium sub-layer. Prior to deposition, pre-sputtering was conducted using a shutter between the target and the substrate, to remove contamination on target surface. The substrate holder was neither rotated nor heated, but cooled down by water circulation. The targets were polished systematically previous to deposition in order to ensure reproducibility. The target to substrate distance was about 5 cm. The adherence of the membranes was checked by the classic adhesive tape test and they showed good adhesion to the substrate. Microscope slides were used as substrates they were cleaned with a commercial detergent in an ultrasonic bath, rinsed in alcohol and dried with dry air. The most important point in the microsensor construction is to ensure a stable on the metal/functional film interface, which is connected with the coating adhesion. The density of the exchange current on the membrane/analyzed solution interface depends on the charge transport mechanism across the glass. The chromium connection helped indeed in improving the continuity of the electrochemical chain. It also helped in increasing the adhesion of the film to the substrate. A wire was attached with a silver micro adhesive. Then the inner side was coated with an epoxy resin.



Fig. 1. RF Sputtering targets. (a) Experimental composite target and (b) Bibliographic prototype [19].

The X-ray Photoelectron Spectroscopy (XPS) spectra were collected using a Surface Science Instruments (S-Probe) spectrometer (model 301). Monochromatised Aluminum  $K\alpha$  radiation ( $h\nu = 1486.6$  eV) was used as the excitation source and a pressure of ca.  $5 \cdot 10^{-8}$  Pa was maintained in the chamber. The apparatus was calibrated by using the photoemission lines of Au (Au 4f(7/2) = 83.9 eV, with reference to the Fermi level) and Cu (Cu 2p(3/2) = 932.5 eV); for the Au 4f(7/2) line the FWHM (full width at half maximum) was 0.86 eV under the recording conditions. The peaks were recorded with constant pass energy of 50 eV. Neutralisation of the surface charge was performed using a low energy flood gun. All the measurements were carried out on thin films. The binding energy scale was calibrated using the C 1s line (284.6 eV) from the carbon contamination.

### 3. Results

Thickness measured at different points of the sputtered nano materials was shown to be maximum at the centre of the films and to decrease as the point moves away from it following the Knudsen's cosinusoidal law. This is a classical result for films deposited by RF sputtering when the substrates are not rotated [12]. Films deposited under the same conditions were characterised by the same thickness at the centre. Thin film composition was controlled by Energy Dispersive Spectrometry (EDS) and Secondary Ion Mass Spectrometry (SIMS) analysis. The reproducibility in composition was checked. The compositions were proved to be reproducible even though they were different from those of the corresponding targets. Even more the compositions were shown to be independent of the film thickness, with variations in composition lower than 2% when the thickness was varied from 50 to 600 nm. Performed EDS analysis showed that deposited films contained 40 at.% of copper. It is demonstrated that the sputtering deposition of  $\text{Cu}_x[\text{Ge.Sb.Se}]_{1-x}$  film was optimized in term of membrane performance when the amount of copper was comprised between 40-60 at.% [19]. The SIMS depth profiles for all the detected positive ions (mass range  $\Delta m = 0 - 180$ ) indicate no change in composition throughout the sample.

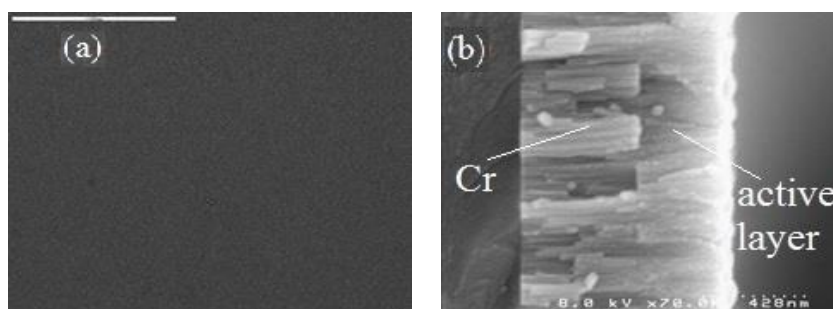


Fig. 2. SEM micrographs. (a) Thin film surface morphology and (b) Cu-Ge-Sb-Se membrane deposited over metallic chromium layer.

In addition to chemical analysis, microstructural and morphological characterisations of the samples have been carried out. Scanning electron microscopy (SEM) analysis has been recorded with a HITACHI S-4500I scanning electron microscope operating at 15 kV. SEM was used to evaluate the homogeneity of composites as well as the quality of the nano materials. Figure 2 indicates that the produced layers have a smooth surface. The membrane surface does not present any defects and secondary phase. The microstructure shows the presence of grains that are probably due to the presence of the columnar structure. The columnar structure of thin films deposited by RF sputtering was highlighted by AFM measurements. The column-like structure can be explained taking into account the Thornton Zone Diagram, the high glass transition temperatures of the chalcogenide materials and the deposition conditions [38]. A columnar structure is observed, whatever the substrate. The average column size and the root mean square (rms) roughness estimated from AFM images measured over an area of few  $\mu\text{m}^2$  were appreciably the same under similar deposition conditions. Note that whatever the argon pressure, a similar columnar structure was observed whatever the composition. As shown in figure 2 images obtained by Scanning Electron Microscopy then confirmed the column-like structure within the layers. On the whole, the data obtained by SEM, EDS and SIMS indicated that the layers were homogeneous and were poorly contaminated. The sensitive membrane has a surface of good quality.

*Table 1. Elemental concentrations at studied films surfaces.*

Elemental concentration (at.%)							sample
Cu	Ge	Sb	Se	O	C	N	
27.3	6.2	6.0	8.3	22.2	30	-	Fresh Sample
13	2.2	2.3	3.5	34	45	-	3 weeks Air exposed
17.8	1.5	3.0	4.2	42	29	2.5	20 days of ageing in Cu(II) solution

Inspection of surface chemistry using high-resolution XPS is one of the most effective ways for optimizing the patterning process [39, 40]. A XPS analysis of the surface was then undertaken in order to get information on the environment of the different elements of the sensing membrane. The analysis of freshly deposited film confirm the the presence of oxygen on the surface as  $\sim 22$  at%. (Table 1). The presence of trace carbon and oxygen at freshly deposited material surface are attributed to surface hydrocarbons adsorbed upon prolonged storage in ambient condition before XPS analysis. Oxygen, when present, exists in various form or physiadsorbed on the Chalcogenide film [40]. Fig. 3 presents the signal of a newly prepared film. it consists of a single peak located at 932.5 eV and corresponding to Cu 2p(3/2). In agreement with previous study the binding energy of the Cu 2p(3/2) photopeak ( $932.6 \pm 0.2$  eV ) corresponds to that of a diamagnetic Cu(I) ions in a selenide environment, type  $\text{Cu}_2\text{Se}$  [7]. We demonstrated elsewhere [2, 5] that The core-level 3d spectra for Se consists of a single peak due to the absence of convolution of the 3d(5/2) and 3d(3/2) peak. The spectrum of the fresh membrane exhibits a broad signal in the range 53–56 eV, corresponding to Se(-II), which has been deconvoluted into two peaks characteristic of two different selenium environments. The one located at 54–56 eV corresponds to  $\text{Cu}_2\text{Se}$  and the one at 53–55 eV to Se bonded to Ge or Sb. Moreover The core-level Se 2p spectra of the fresh membrane consists of a doublet corresponding to the 2p(3/2) and 2p(1/2) peaks of Se. The doublet is located between 160.5 and 166 eV with a peak separation of 5.64 eV, corresponding to Se(-II). On the other hand the Ge 3p(3/2) and the Ge 3d (Fig. 4) was found at a binding energies of 124.0 eV and 32.4 eV respectively. These results show that the Ge is in an environment  $\text{GeSe}_2$ . Further investigation (not shown) indicate the Sb 3d(5/2) peak at 530.4 eV and the Sb 3d(3/2) peak at 539.8 eV.

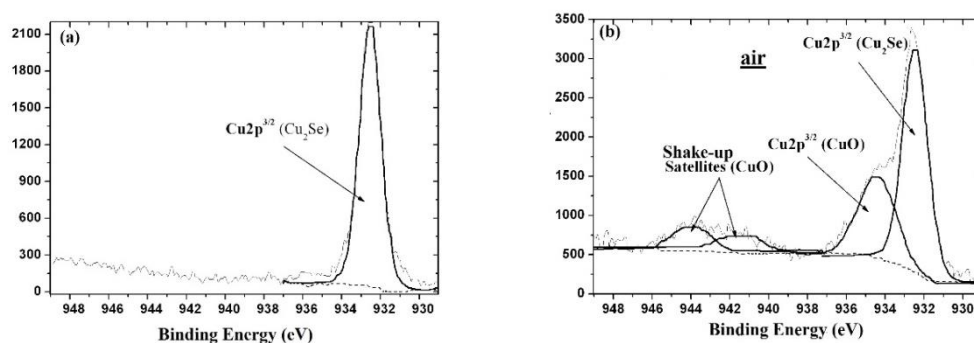


Fig. 3. XPS spectra of the Cu 2p. (a) Untreated membrane, (b) 3 weeks air exposed membrane.

The Sb 3d(5/2) and Sb 3d(3/2) spin-orbit split components for a fresh ISE membrane are most likely attributed to an  $\text{Sb}_2\text{Se}_3$  species (and probably some  $\text{Sb}_2\text{O}_3$ ) [5] noting that Sb 3d revealed a single species. As shown in Fig. 4 it is in agreement with a broad signal in the range 34–36 eV which has been deconvoluted into two peaks [i. e. Sb 4d(5/2) and Sb 4d(3/2)]. It is important to note that the Sb 3d level for  $\text{Sb}_2\text{Se}_3$  and  $\text{Sb}_2\text{O}_3$  have similar binding energies. The formation of elemental antimony (i.e. Sb(0)) or an antimony species of higher oxidation state (i.e.  $\text{Sb}_2\text{O}_5$ ) was not evident. The Ge 3d binding-energy shoulders are consistent with the formation of  $\text{GeO}_2$  [2]. It is important to note that the Ge spectra did not reveal a peak corresponding to elemental germanium. After the deposition, an oxidation process (i.e. 3 weeks air exposure) was conducted by exposing  $\text{Cu}_x(\text{Ge}_{28}\text{Sb}_{12}\text{Se}_{60})_{1-x}$  samples to air at room temperature. The oxidized surfaces of the samples were then studied by XPS. The core level spectra acquired from oxidized membrane surfaces were deconvoluted by using appropriate software [2, 5, 7]. For the exposed-to-air samples, the O content detected on the surfaces became higher. For each compound, an oxygen atomic percentage has been found at the fresh membrane surface (i.e. 22.2 at. % of O), it increases after air exposure (i.e. 34 at. % of O). The increase in O content could be attributed to O-affinity of chalcogenide surface [41]. Further analysis are made for O 1s and C 1s spectra. As can be seen in Table 2 the O 1s spectra after oxidation process, is composed of three components which represent signals from oxygen in oxide ( $\text{O}^{2-}$ ) at BE of 530.6 eV, water at BE of 532.5 eV and carbon-oxygen bonds at BE of 534.1 eV [40]. Similarly, the C 1 spectra consist three components, at BE of 286.4 eV, 287.4 eV and 289.2 eV (the first one is connected with carbon contamination while the next two represent the carbon-oxygen bonds [39, 40]).

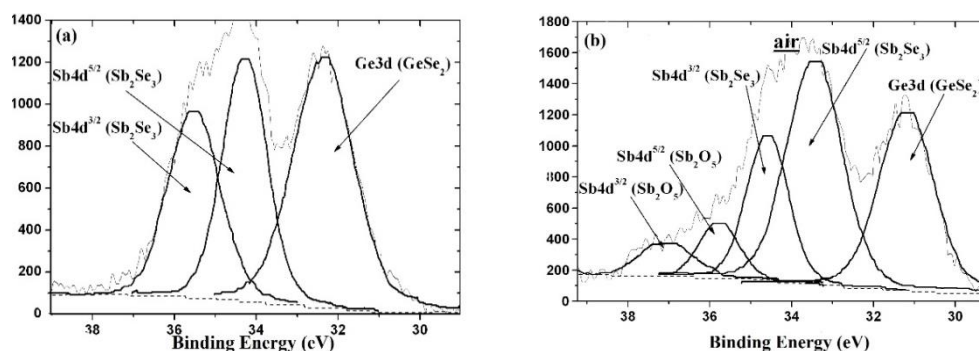


Fig. 4. XPS spectra of Sb 4d. (a) Untreated membrane, (b) 3 weeks air exposed membrane.

As shown in Table 1, quantitative XPS analysis revealed a variation in the surface atomic ratios. In particular, it was found that the Se/Ge atomic ratio increased after oxidation process at room temperature (i.e. Se/Ge atomic ratio of 1.3 before air exposure, rising to 1.6 after 3 weeks of air treatment). Moreover, the O/Sb ratio displayed a steady increase, whereas the O/Ge and O/Sb ratios are close to same value. Nevertheless, the absence of Se–O bonds indicates that the

oxidation of selenium does not occur, but rather the substitution of oxygen atoms for selenium atoms takes place. XPS investigation reveals that an interaction of the freshly prepared films with air at room temperature during 3 weeks caused the partial oxidation of the copper at the surface. The XPS spectra of air treated thin films are shown in Fig. 3. They comprised a broad signal in the range 931–937 eV attributed to Cu 2p(3/2). The signal can be deconvoluted into two peaks, one located at 932.5 eV similar to the one observed in the spectrum of the fresh membrane and one at 934.2 eV corresponding to Cu bonded to O, type CuO. An additional signal in the range 940–945 eV,  $\pm 9$  eV higher than the energy of the main 2p(3/2) peak, is also observed in the spectra. It is attributed to the high-intensity shake-up satellites. At the same time a large peak appeared in the range 34–39 eV (Fig. 4). It corresponds to Sb bonded to O, type Sb(V) [23]. This signal consists of a single peak due to the absence of convolution of the 4d(5/2) and 4d(3/2) peaks. Moreover Sb 3d(3/2) peak located at 541,8 eV confirms the presence of antimony species of higher oxidation state (i.e. Sb<sub>2</sub>O<sub>5</sub>) at sensing membrane surface.

Table 2. The XPS binding energies (ev) of studied films.

	Level	Untreated	3 weeks air exposed	20 days age in 10 <sup>-4</sup> M Cu(NO <sub>3</sub> ) <sub>2</sub>
Cu <sub>2</sub> Se	Cu 2p3/2	932.5	932.5	932.5
CuO	Cu 2p3/2	ND	934.2	934.7
Se <sup>-2</sup>	Se 2p3/2	160.5	160.8	160.8
	Se 2p1/2	166	-	-
SeO <sub>3</sub> <sup>-2</sup>	Se 2p3/2	ND	ND	164.8
GeSe <sub>2</sub>	Ge 3p3/2	124.0	-	-
	Ge 3d	32.4	31.3	32.1
Sb <sub>2</sub> O <sub>3</sub>	Sb 3d5/2	530.4	-	-
	Sb 3d3/2	539.8	538.9	540.1
Sb <sub>2</sub> O <sub>5</sub>	Sb 3d3/2	ND	541.8	ND
C	C 1s	284.6	286.4	284.6
		-	287.4	286.2
		-	289.2	288
O	O 1s	-	530.6	-
		-	532.5	-
		-	534.1	-

It is of interest to note that the oxidation process is not followed by any perceptible changes in the chemical state of the Ge and Se elements. No shift in binding energy for the Se 3d, Se 2p, Ge 3d and Ge 3p peaks is observed. It is clearly evident that studied oxidation process is different from ageing process in copper nitrate solution. We demonstrated elsewhere that the chemical composition of the membrane is modified as soon as the membrane is soaked in a copper (II) solution and its alteration corresponds to an oxidation of copper and selenium at the membrane surface and a dissolution of the chalcogenide glassy matrix in the copper nitrate solution [7]. It is to be note that oxidation is less strong at the sensing membrane surface after 3 weeks air exposure than after 20 days of ageing in Cu(NO<sub>3</sub>)<sub>2</sub> 10<sup>-4</sup> M solution. Further experiments are then in progress in order to study influence of storage condition on sensor electrochemical behavior.

#### 4. Conclusions

The X-ray Photoelectron Spectroscopy analysis of Cu-ISE surface was done in order to study air-ageing of the sensing membrane. As one can expect, the XPS measurements give a clear evidence that the surfaces of the oxidised air-exposed samples are composed mainly of oxygen and carbon. Air-ageing at room temperature confirms the presence of Sb<sub>2</sub>O<sub>5</sub> species at sensing device surface with a less strong oxidation process than ageing in copper solution. According to the

oxidation rate the results suggested that air-storage at room temperature involve a great ISE life time. In order to understand oxidation mechanism Electrochemical Impedance Spectroscopy experiments are in progress. The very first EIS data are internally consistent with XPS results

## References

- [1] M. Essi, *Chalcogen. Lett.* **8**, 301 (2011).
- [2] F. O. Méar, M. Essi, P. Siatat, P. Huguet, A. Pradel, M. Ribes, Proc. in the 21st Inter. Conf. On Solid Waste Technol. and Managent (ICSWM), Philadelphia, PA (USA), 2006.
- [3] V. Thiago Moreno, G. C. Nelson Astrath, *J. Non-Cryst. Solids* **495**, 8 (2018).
- [4] Rudnitskaya, I. Delgadillo *Sens. Actuators B* **238**, 1181 (2017).
- [5] F. O. Méar, M. Essi, M.-F. Guimon, A. Pradel, *Chalcogen. Lett.* **5**, 117 (2008).
- [6] R. De Marco, J. Martizano, *Talanta* **75**, 1234 (2008).
- [7] F. O. Méar, M. Essi, P. Siatat, M.-F. Guimon, D. Gonbeau, A. Pradel, *Appl. Surf. Sci.* **255**, 6607 (2009).
- [8] M. Essi, *Chalcogen. Lett.* **8**, 25 (2011).
- [9] M. Maric, M. Sohail, J. P. Veder, R. De Marco, *Sens. Actuators B* **207**, 907 (2015).
- [10] M. Essi, A. Pradel, *Chalcogen. Lett.* **8**, 15 (2011).
- [11] P. Salazar, M. Martín, R. Ford, R. D. O'Neill, J. L. González-Mora, *Encyclopedia of Interfacial Chemistry*, 374 (2018).
- [12] M. Essi, P. G. Yot, G. Chevallier, C. Estournes, A. Pradel, *Dig. J. Nanomater. Bios* **6**, 1777 (2011)
- [13] J. Charrier, M. L. Brandily, V. Nazabal, *Sens. Actuators B* **173**, 468 (2012).
- [14] Yu. G. Vlasov, E. A. Bychkov, *Ion-Selective Electrode Rev.* **9**, 3 (1987).
- [15] Yu. G. Vlasov, E. A. Bychkov, B. L. Seleznev, *Solid State Ionics* **24**, 179 (1987).
- [16] Yu. G. Vlasov, E. A. Bychkov, B. L. Seleznev, *Sens. Actuators B* **2**, 23 (1990).
- [17] Yu. G. Vlasov, E. A. Bychkov, A. M. Medvedev, *Anal. Chim. Acta* **185**, 137 (1986).
- [18] R. Svoboda, J. Malek, *Handbook of Thermal Analysis and Calorimerty* **6**, 487 (2018).
- [19] G. Taillades, O. Valls, A. Bratov, C. Dominguez, A. Pradel, M. Ribes, *Sens. Actuators B* **59**, 123 (1999).
- [20] C. Cali, G. Taillades, A. Pradel, M. Ribes. *Sens. Actuators B* **76**, 560 (2001).
- [21] A. Guessous, J. Sarradin, P. Papet, K. Elkacemi, S. Belcadi, A. Pradel, M. Ribes, *Sens. Actuators B* **53**, 13 (1998).
- [22] Y. Mourzina, M. Schöning, J. Schubert, W. Zander, A. Legin, Y. Vlasov, H. Luth, *Anal. Chim. Acta* **433**, 103 (2001).
- [23] Yu. Mourzina, M. J. Schöning, J. Schubert, W. Zander, A. V. Legin, Yu. G. Vlasov, P. Kordos, H. Lüth, *Sens. Actuators B* **71**, 13 (2000).
- [24] V. Vassilev, K. Tomova, S. Boycheva, *J. Non-Cryst. Solids* **353**, 2779 (2007).
- [25] C. T. Baker, I. Trachtenberg, *J. Electrochem. Soc.* **118**, 571 (1971).
- [26] R. Jasinski, I. Trachtenberg, G. Rice, *J. Electrochem. Soc.* **121**, 363 (1974).
- [27] S. P. Awasthi, N. S. Shenoy, T. P. Radhakrishnan, *Analyst* **119**, 1361 (1994).
- [28] J. Schubert, M. J. Schoning, C. Schmidt, M. Siegert, St. Mesters, W. Zander, P. Kordos, H. Luth, A. Legin, Yu. G. Mourzina, B. Seleznev, Yu. G. Vlasov, *Appl. Phys. A Mater. Sci. Process* **69**(7), 803 (1999).
- [29] A. E. Owen, *J. Non-Cryst. Solids* **35–36**, 999 (1980).
- [30] N. Tohge, M. Tanaka, *J. Non-Cryst. Solids* **80**, 550 (1986).
- [31] M. I. Frazer, A. E. Owen, *J. Non-Cryst. Solids* **59–60**, 1031 (1983).
- [32] Yu. G. Vlasov, E. A. Bychkov, A. M. Medvedev, *Zh. Anal. Khim.* **40**, 438 (1985).
- [33] M. J. Schoning, C. Schmidt, J. Schubert, W. Zander, S. Mesters, P. Kordos, H. Luth, A. Legin, B. Seleznev, Yu. G. Vlasov, *Sens. Actuators B* **68**, 254 (2000).
- [34] R. Tomova, G. Spasov, R. Stoycheva-Topalova, A. Buroff, *J. Non-Cryst. Solids* **266–269**, 985 (2000).
- [35] M. Essi, *Chalcogen. Lett.* **8**, 341 (2011).
- [36] M. Essi, *Journal of Non-Oxide Glasses* **3**, 8 (2011).

- [37] M. Essi, *Chalcogen. Lett.* **8**, 103 (2011).
- [38] V. Balan, C. Vigreux, A. Pradel, A. Llobera, C. Dominguez, M. I. Alonso, M. Garriga, J. Non-Cryst. Solids **326-327**, 455 (2003).
- [39] R. Idczak, K. Idczak, R. Konieczny. *Phys. B* **528**, 27 (2018).
- [40] C. Chantharangi, C. Paksunchai, S. Denchitcharoen, S. Chaiyakun, P. Limsuwan. *Materials Today: Proceedings* **5**, 15155 (2018).